# Comparison between salt crystallization weathering test and natural weathering in Mesozoic's anisotropic rocks, a case study: Arakʾs Calcareous slates, Iran

**Parya Behzadtabar [1]\*, Mohammad Hossein Ghobadi [1], Davood Fereidooni [2]**, Ali Asghar Sepahi [1]

[1] *Department of Geology, Bu-Ali Sina University, Hamadan, Iran*

[2] *School of Earth Sciences, Damghan University, Damghan, Iran*

*\*Corresponding author, e–mail: p.behzadtabar@yahoo.com*

(*received: 25/06/2018 ; accepted: 30/01/2019*)

**Abstract**

Salt crystallization can severely damage anisotropic foliated rocks, therefore it is necessary to have an understanding of crystallization process. The present study was conducted to investigate the effect of salt crystallization on Arakʾs calcareous slates, as anisotropic rocks of Mesozoic. To compare salt crystallization weathering (*EN* 12370 norm was used up to 30 cycles) with natural weathering conditions, some samples were exposed to natural weathering conditions for 12 months. The samples exposed natural condition were tested every 3 months. The measurements show a decrease in physical and strength properties with an increase salt crystallization cycles. At the end of cycle 30, the average weight, ultrasound wave velocity, uniaxial compressive strength ($\sigma_c$), Brazilian tensile strength ($\sigma_t$), and point load index value ($I_s$) of the samples were reduced by 0.32%, 11.52%, 23.72%, 32.15%, and 16.09%, respectively. In comparison, after about 12 months of exposure to natural climatic conditions, these values were 0.18%, 8.84%, 12.64%, 22.23%, and 15.04%, respectively. To establish a relationship between salt crystallization and natural weathering conditions, weathering ratio (*WR*) was presented. The results of this study can be used to predict the behavior of the anisotropic slates of Arak, upon which the city is planned to be developed.

**Keywords**: *Salt crystallization, Natural weathering, Anisotropy, Calcareous slate, Arak.*

## Introduction

Salts degrade strength properties of building materials and foundation. Soluble salts are recognized as important weathering agents in dry environments close to the seas. In these environments, salts contain various components such as $Na_2SO_4$, $MgSO_4$, *and NaCl*. As the stone dries out, the evaporation of the solvent results in an increase in the salt concentration of the residual solution, so that the salt possibly solidifies wherever the concentration goes beyond the supersaturation threshold locally required for crystallization.

Various investigations have been conducted regarding effect of salt crystallization on construction stones and building materials (e.g., Zedef *et al*., 2007; Lourens *et al.,* 2005; Koniorczyk & Gawin, 2012; Modestou *et al.,* 2015; Stryszewska & Kanka, 2017). In recent investigations, several theoretical and laboratory studies have been conducted to determine properties of anisotropic rocks have been undertaken by many researchers (Fereidooni *et al.,* 2016; Khanlari *et al.,* 2014; Ikari *et al.,* 2015; Heng *et al.,* 2015).

Dissolved sodium sulfate (*2Na, SO2⁻₄*) can crystallize as either an anhydride crystal (thenardite) or a hydrated crystal (mirabilite).

Olivier Coussy (2006) explained that crystallization of sodium sulfate (thenardite or mirabilite) depends on environmental conditions including temperature and relative humidity. It has to be noted that thenardite remains stable only at T>34℃, below which it transforms to mirabilite by a dissolution-precipitation process.

Crystallization of the porous systems typically occurs near to the surfaces and leads to the decay of stones. This damage caused by crystallization (subflorescence) is preferentially observed for sodium sulfate (Rodriguez-Navarro & Doehne, 1999; Cardell *et al.,* 2003). In fact, in the sodium sulfate solution, the slower capillary flow permits a more significant evaporation within the material and results in subflorescence (Rodriguez-Navarro & Doehne, 1999).

There are few studies on the effects of natural weathering on rocks because it needs a longer time than accelerated laboratory weathering tests. Gautam & Shakoor (2013) studied on slaking behavior of clay-bearing rocks during a one-year exposure to natural climatic conditions. They reported that siltstones are the most durable rocks under natural climatic conditions since they remain mostly intact during the first 3 months of exposure and then slake slowly and slightly through the

development of cracks.

As a result of increasing population and industrialization in the recent decades, Arak (a city in Iran) has faced several environmental and engineering problems. The engineering problems are especially degradation of strength and durability of building materials and foundations. In addition to daily construction activities, the Arakꞌs slate-rocks have highly been used as building stones and foundations. The main aim of the present study is to assess the physical and mechanical alterations of anisotropic slates of Arak due to salt crystallization test and natural weathering processes. Finally, comparing the laboratory salt crystallization weathering process with weathering in natural conditions, and and suggesting a relationship between these.

**Materials and methods**
In general, the preparation of the test specimens, their dimensions, and the minimum number of the specimens are essential to establish the properties of rocks based on the applied method. In this work, slate blocks of three stations (*N*, *M*, and *G*) were chosen (Fig. 1a) and moved to the laboratory. Then, the weathering and mechanical tests were carried out on cylindrical specimens with a diameter of 54 mm according to the methods suggested by *ISRM* (2007) and *ASTM* (2000) recommendations. The sampling procedure followed for specimens' preparation for mechanical tests is illustrated in Fig 1b.

Mineralogical, textural, and physical properties including dry density ($\gamma_d$), saturated densities ($\gamma_{sat}$), submerged density ($\gamma_{sub}$), water absorption ($W_a$), porosity (*n*), and specific gravity ($G_s$) were determined for the rock samples of the three stations. Mechanical properties including uniaxial compressive strength (*UCS*), point load strength (*PLT*), and Brazilian tensile strength (*BTS*) were determined from the core specimens The *ISRM* (2007)-suggested methods were used to determine physical and mechanical properties of the rocks. $Na_2SO_4$ and *NaCl* are the main constituents of the

Arakꞌs brine (Ghadimi *et al.,* 2013), therefore, sodium sulfate was used for salt cey test. The procedure followed for salt crystallization is described in the *EN* 12370 norm (2001). Specifically, specimens were undergone 30 cycles consisting of 1) 2 h of immersion in a supersaturated solution of sodium sulfate (14% w/w at 20℃); 2) 16 h of drying in an oven at 105℃; and 3) 6 h of cooling at room temperature. The samples were exposed to 30 cycles of salt crystallization. Then, at cycles 10, 20, and 30, the samples were extracted and tested. Sodium sulfate is typically selected for two reasons: First, it is very common in a wide range of locations and environments and, second, it is extremely destructive (Rodriguez-Navarro *et al.,* 2000)

To compare salt crystallization weathering with natural weathering condition, the samples were placed on a roof (Fig. 2) of Hamadan city, where the weather conditions (apart from air pollution) are almost same to those of Arak, and exposed to natural climatic conditions from April 2017 to April 2018 (Table1). At the end of each 3 months (90 days), 15 samples (of every station) were tested, where they experienced all three climatic cycles (heating and cooling, wetting and drying, and freezing and thawing). Finally, all results were analyzed.

**Results**
*Petrographic and physical properties*
Petrographic parameters play a key role in controlling the weathering of rocks. The main property of slates is their ability to splitting. There are several geological processes that cause this property (*e.g.,* sedimentation, folding, and cleavage). The trace of these processes is found in the microscopic fabric of the slate. Accurately identifying this microscopic fabric will make it possible to recommend the best use for a particular variety of slate. Slates are defined as rocks with minerals not visible to the naked eye or even with a hand lens, slaty cleavage, and a dark color.

Table1. The characteristics of weathering cycles in natural conditions

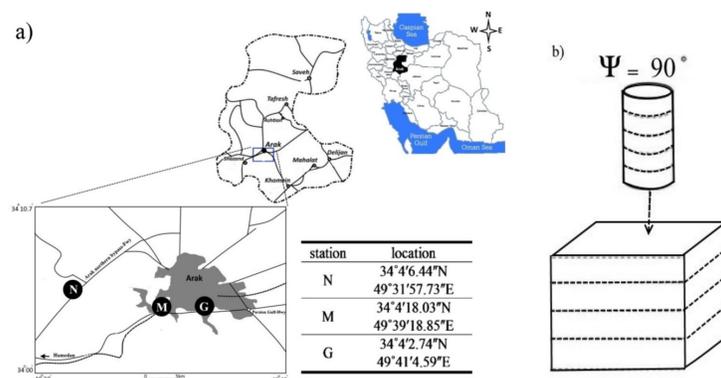| Cycle number | Period (day) | Thaw-Freeze (day) | Wet – Dry (day) | Warm – Cold (day) | average minimum temperature | Average maximum temperature |
|---|---|---|---|---|---|---|
| **1** | 90 | 0 | 17 | 73 | 9 | 26/7 |
| **2** | 180 | 0 | 18 | 162 | 10 | 30 |
| **3** | 270 | 5 | 28 | 237 | 7 | 25 |
| **4** | 360 | 22 | 48 | 290 | 5 | 23 |

Figure 1. a) Location of the sampling stations, b) Directional coring diagram of the specimens



Figure 2. Slate cores exposed to natural climatic conditions

The petrography of most of the roofing slates is rather simple. The main minerals are quartz, mica, and chlorites, with a lepidoblastic texture (Ward & Gómez-Fernandez, 2003; Walsh, 2007). Other minerals can be easily found but in minor quantities; e.g., feldspar (albite), chloritoid, carbonates, iron sulfides, rutile, tourmaline, zircon, and biotite (Cárdenes *et al.,* 2014). The thin sections and *XRD* (X-ray Diffraction) test results showed chlorite-sericite, quartz, calcite, pyrite-magnetite, and graphite (tree stations in same). Platy minerals such as chlorite, basically consisting of extended flat sheets of linked silicates, display a flat or flaky crystal habit or a planar cleavage.

In some slates, it is also possible to find limestone fragments (Cárdenes *et al.,* 2010) such as those found in the samples studied. These fragments could have a negative effect on rocks' durability and strength.

The main texture of the samples is lepidoblastic (fine grained), in which few coarse-grained chlorite and pyrite-magnetite (Porphyro-lepidoblastic) exist. The presence of minerals that are vulnerable to weathering like iron sulfides and carbonates is not desirable in slate (Cárdenes *et al.,* 2012a). Low metamorphosis causes clay mineral (chlorite) to arrange and leads to creating graphite. Presence of non-dissolved minerals such as graphite in rocks decreases Unconfined Compressing Strength (*UCS*) but increases the slake durability index (Fereidoni & Ghobadi, 2015).

As can be seen from Fig. 3, calcite vines, which lie perpendicular to foliation, in station *M* are more than those in stations *N* and *G*. Infiltration *CO₂*-rich

solutions are the reason for the formation of these veins, which lead to decreasing resistance and durability.

Diamantis *et al.* (2014) demonstrate that the physicomechanical characteristics are strongly influenced by the petrographical characteristics except for mineral grain size. In addition, rocks with various petrographies represent different weathering rates in similar climatic conditions

(Momeni *et al.,* 2015; Heidari *et al.,* 2017). Table 2 presents the measured saturated and submerged unit weights ($\gamma_d$, $\gamma_{sat}$, and $\gamma_{sub}$), specific gravity ($Gs$), porosity ($n$), and water absorption ($Wa$). According to the classification of dry density and porosity (Anon, 1974), the studied samples' porosities fall in Class 4 (low) and their densities fall in Class 5 (very high).

Table 2. Average value of physical properties of the rock samples

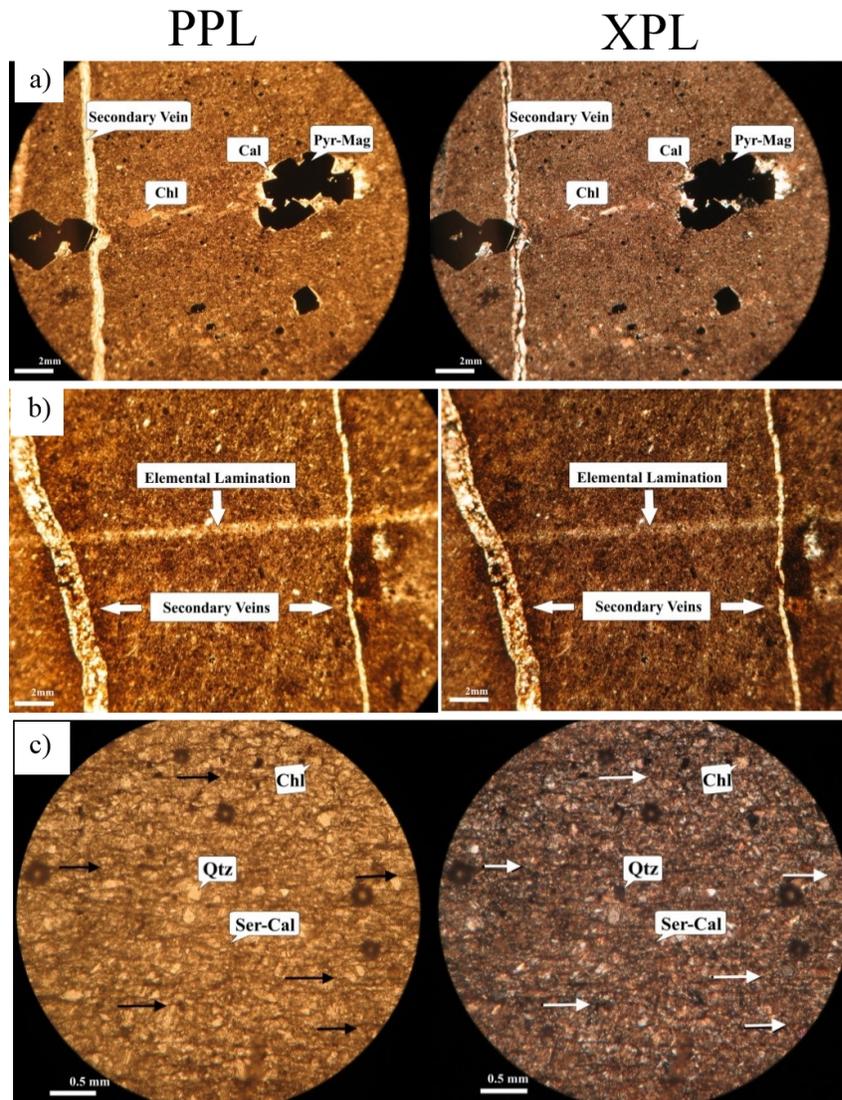| Station | $\gamma_d$ (g/cm³) | $\gamma_{sat}$ (g/cm³) | $\gamma_{sub}$ (g/cm³) | $G_s$ | $n$ (%) | $W_a$ (%) |
|---|---|---|---|---|---|---|
| G | 2.87 | 2.87 | 1.81 | 2.89 | 0.71 | 0.26 |
| N | 2.86 | 2.87 | 1.86 | 2.92 | 2.21 | 0.82 |
| M | 2.78 | 2.8 | 1.75 | 2.84 | 2.2 | 0.81 |



Figure 3. Photomicrographs of rock samples: a) Station N (parallel to the foliation), b) Station *M* (parallel to the foliation), and c) Station *G* (perpendicular to the foliation) (*Cal*: Calcite, *Qtz*: Quartz, *Chl*: Chlorite, *Pyr-Mag*: pyrite-Magnetite, and *Se*r: seresite).

The dry unit weights of the rocks were high, but the values of porosity and water absorption were low. Fereidooni (2014) suggested that porosity is the most important factor influencing ultrasonic wave velocity of the rocks. In the rocks, the dry unit weights are mainly controlled by dense minerals such as garnet and, thus, are affected by porosity. The physical and mechanical effects due to salt crystallization on slates were measured under the laboratory conditions. For this purpose, dry weight loss (*DWL*), P-wave velocity (*Vp*), uniaxial compressive strength ($\sigma_c$), Brazilian tensile strength test ($\sigma_t$), point load index (*Is*) were accomplished.

*Observable changes during to salt crystallization cycles*

Aesthetics of slates are very subjective and depend on each customer's preference. In this regard, the minimum degree of homogeneity in appearance is necessary, even for heterogeneous materials (Cárdenes *et al.,* 2014). Although the main property of any slate is its ability to splitting, this property is problematic. In fact, when the slate is used as a building material in the foundation, its splitting is a negative point, especially when it is exposed to weathering.

In sodium sulfate crystallization, anhydrous sodium sulfate precipitation is promoted in micropores due to water activity reduction. Fast evaporation and the high degree of solution supersaturation reached in micropores before thenardite precipitation result in high crystallization pressure generation and a greater damage to porous materials than mirabilite (Rodriguez-Navarro *et al.,* 2000). In our test conditions, which involve high evaporation rate conditions (drying at 105℃), it resulted in the crystallization of sub-fluorescence (*i.e.,* crystals formed inside the stone pores). In these conditions, the evaporation front located some distance from the stone surface and formed up to 4 mm-thick. However, after a certain number of cycles, this thickness increases. Low porosity of slates caused penetration depth of salt to be limited to weak planes, leading to some good illustration such as veins and foliation. Hence, the penetration depth of weathering declines and its evidence is more visible at the surface (Fig 4). In addition, salt crystallization cycles caused foliation to separate (Fig. 5). This issue causes physical and mechanical properties to switch.

Apparent features of the samples alteration for cycle 10 are corrosion of peripheral edges, development of foliation's line due to color changes (Fig. 6a) at cycles 20 and 30, color changes in pyrite-magnetite grains, corrosion of peripheral edges, and appearing foliation line due to exudation (Fig. 6 b and Fig. 6c).

Iron sulfide oxidation and gypsification are two main degrading factors in the weatherability of slate are (Walsh, 2008; Cárdenes *et al.,* 2012a). Iron sulfide oxidation is seen as pale stains (Fig. 6d). According to Cárdenes et al. (2014), the iron sulfide oxidation generates streams of reddish oxide that run across the roof surface, affecting the surface's appearance, but usually without compromising the water proofing of the roof.

Zedef *et al.* (2007) reported that a decrease in *CaO*, *MgO*, and *FeO* oxides reduces weathering intensity. They reported that as the intensity of weathering increases, *Ca*, *Na* and *K* contents of clay minerals such as illite-smectite, kaolinite and chlorite, which are the main product of alteration, indicate a decrease.
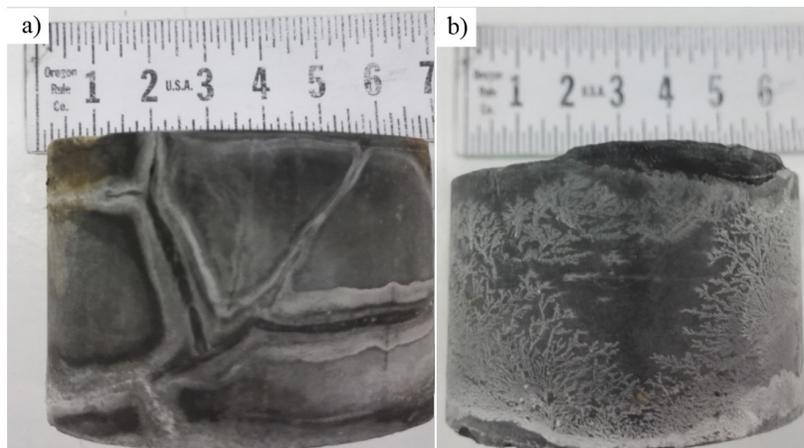


Figure 4. Effect of weak planes on the penetration depth of salt: a) a jointed slate and b) an intact slate
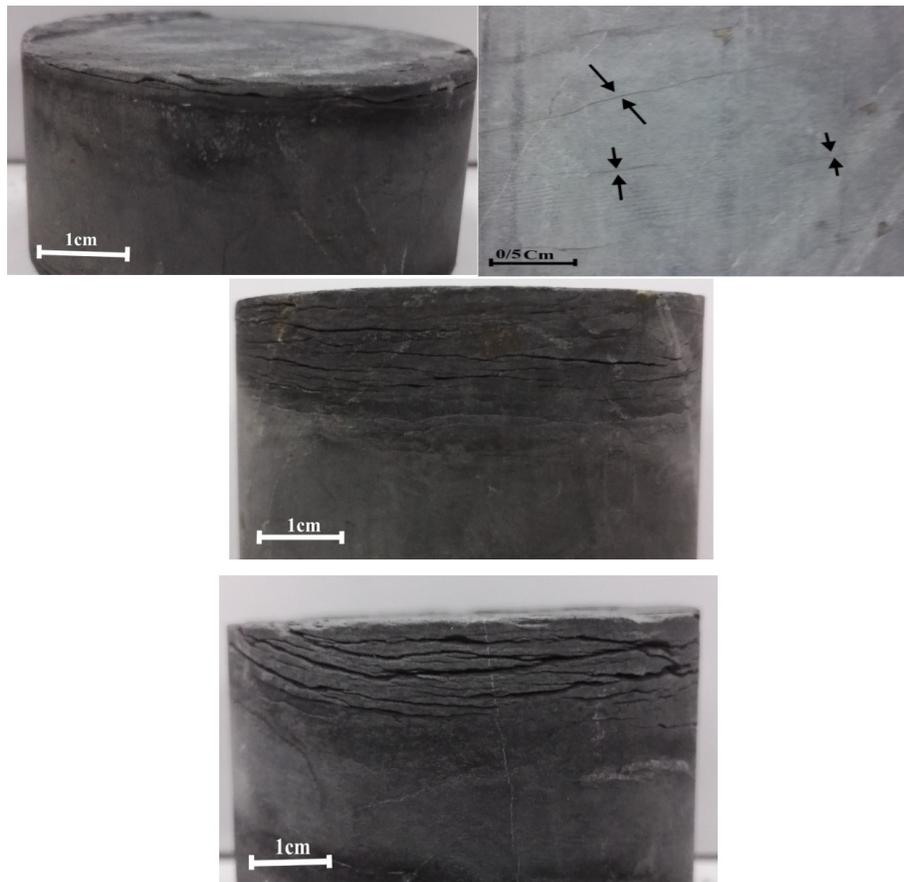
Figure 5. Visible changes on foliation due to salt crystallization cycles (10, 20, and 30).
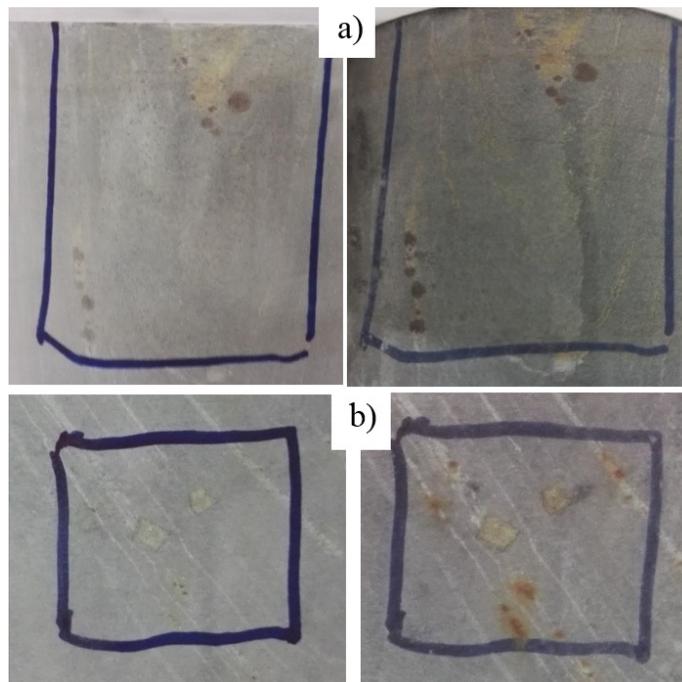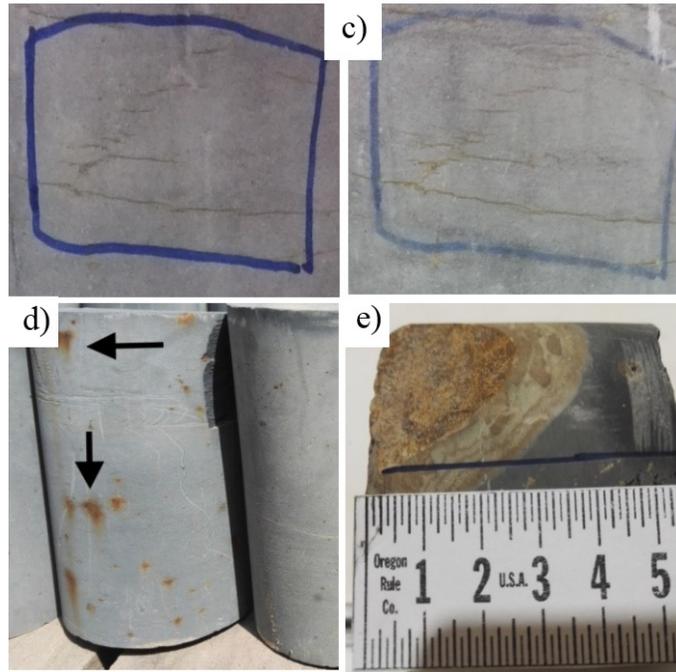
Figure 6. To be continued

Figure 7. Observable changes due to weathering: a) cycles 10, b) cycles 20, c) cycles 30, d) short-term natural weathering, and e) long-term natural weathering condition

Gypsification, in Arak's slates (Fig. 6e), is detected in the form of discoloration (dark grey in fresh color to milky in the weathered surface). The gypsification is the process by which gypsum crystals are formed as a result of the weathering of the carbonate minerals.

Presence of a larger amount of gypsum than carbonate leads to a softening and destruction of the slate's fabric and decreasing its general resistance to weathering. In this regard, passivation techniques have been proposed to prevent this oxidation (Cárdenes *et al.,* 2009) and shown promising results. Also, the use of protective products (siloxanes) has been tested in slate tiles (Rivas *et al.,* 2011).

*Results of salt crystallization test*
The results of physical and mechanical tests are reported in Figs. 7-11. All physicomechanical tests were carried out on 15 samples in each weathering cycle for each station (totally 135 samples). In the first step, dry weight loss (*DWL*) and ultrasound wave velocity index (*DV_p*) according were determined according to Eqs. 1 and 2, respectively:

$$DWL(\%) = \left(\frac{W0 - W1}{W0}\right) * 100 \qquad \text{Eq. 1}$$

$$DVp(\%) = \left(\frac{V0 - V1}{V0}\right) * 100 \qquad \text{Eq. 2}$$

Where $W_0$ is initial dry weight, $W_1$ is secondary dry weight (in cycles 10, 20 and 30), $V_0$ is initial wave velocity, and $V_1$ is secondary wave velocity (at the end of cycles).

As can be seen in Figs. 7 and 8, for all samples, with increasing the number of cycles, dry weight and ultrasound wave velocity were reduced, due to the increase in the intensity of exfoliation and corrosion. Station *M* shows the highest weight decline compared with these in stations *N* and *G*, which is directly associated with density ($\gamma_G > \gamma_N > \gamma_M$).



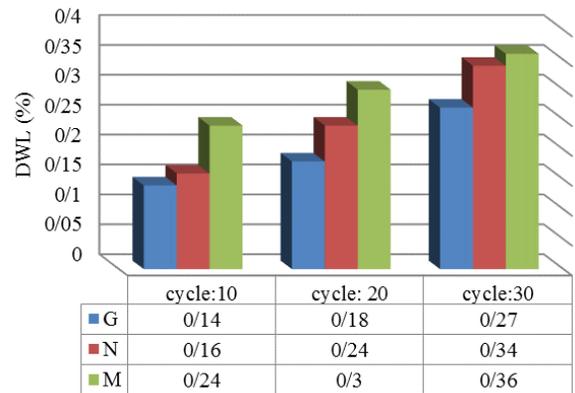|  | cycle:10 | cycle: 20 | cycle:30 |
|---|---|---|---|
| ■ G | 0/14 | 0/18 | 0/27 |
| ■ N | 0/16 | 0/24 | 0/34 |
| ■ M | 0/24 | 0/3 | 0/36 |

Figure 8. Dry weight loss (DWL) against cycle (C) in stations (G, N, M, and their average)
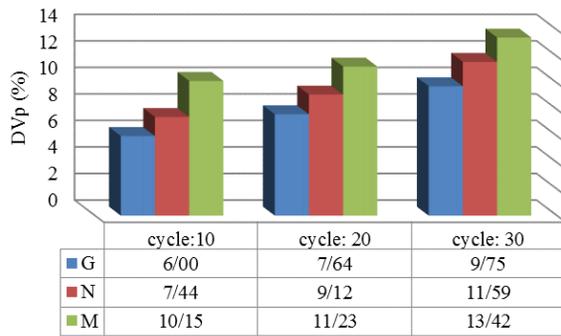
Figure 9. Ultrasound wave velocity index (DVp) against cycle (C) in stations (G, N, M, and their average)

Olivier Coussy (2006) acknowledged that, owing to intermolecular forces and to the associated disjoining salt solution pressure, a thin layer of aqueous solution always remains between the crystal and the internal solid walls of the porous network. This thin layer facilitates the further in-pore crystallization by allowing the solute to diffuse to the previously crystallized sites.

Using the exponential function, a decrease in tensile and compressive strengths and point load index were observed in all stations. Changes trend, as expected, was a function of slate density (Figs. 9-11).

The equations presented in Figs. 7-11 could be used for predicting calcareous slates behaviors under salt crystallization test.

As discussed in Sections 3-5, the average equations (Eqs. 6, 10, and 14) were used for estimating strengths for long test periods (in this case 90, 180, 270, and 360 cycles) and comparing with natural weathering condition.
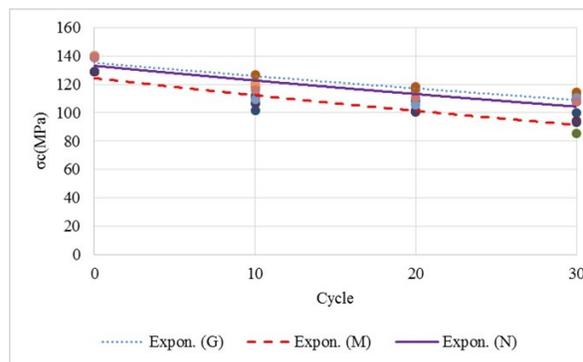


| Station | Eq. Number | Eq. | R² |
|---------|-----------|-----|-----|
| G | 3 | $\sigma c = 135.6e^{-0.007C}$ | 0.87 |
| M | 4 | $\sigma c = 124.35e^{-0.01C}$ | 0.92 |
| N | 5 | $\sigma c = 133.1e^{-0.008C}$ | 0.83 |

Figure 9. Uniaxial compressive strength (σc) against the number of cycles (C) and their equations in stations (G, M and N).
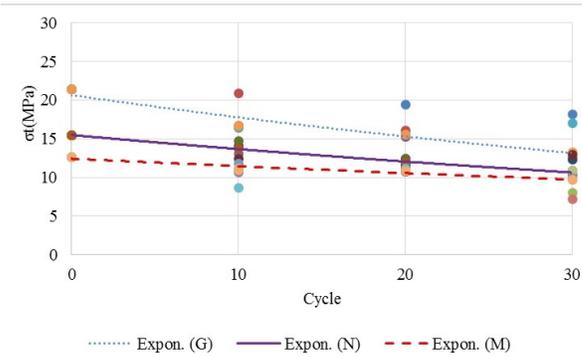


| Station | Eq. Number | Eq. | R² |
|---------|-----------|-----|-----|
| G | 7 | $\sigma t = 20.789e^{-0.015c}$ | 0.96 |
| M | 8 | $\sigma t = 12.424e^{-0.008c}$ | 0.90 |
| N | 9 | $\sigma t = 15.481e^{-0.013c}$ | 0.99 |

Figure 10. Tensile strength (σt) against the number of cycles (C) and their equations in stations (G, M and N).



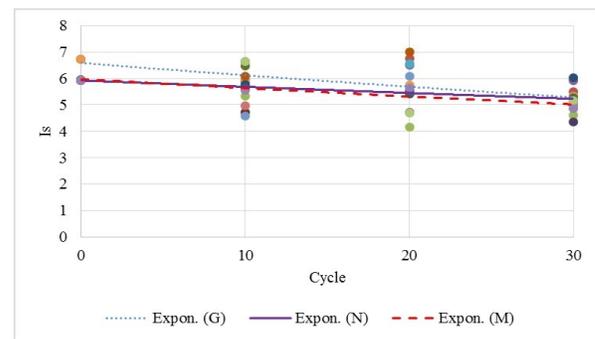| Station | Eq. Number | Eq. | R² |
|---------|-----------|-----|-----|
| G | 11 | $Is = 6.591e^{-0.007c}$ | 0.93 |
| M | 12 | $Is = 5.91e^{-0.005c}$ | 0.98 |
| N | 13 | $Is = 5.9267e^{-0.004c}$ | 0.99 |

Figure 11. Point load index (Is) against the number of cycles (C) and their equations in the station (G, M and N)

There is a strong relationship between slate fabric and mechanical behavior. Because the slate in station *G* is fine-grained than other stations, it also showed higher strengths. As Cárdenes *et al.* (2012) explained that a slate with fine-grained and homogeneous fabrics usually has a higher bending strength.

*Natural Weathering Condition (NWC)*
To study natural weathering condition, the samples were exposed to natural climatic conditions from April 2017 to April 2018 (12 months). Every 3 months, one group of the sample from each station was removed from natural exposure and their physicomechanical properties were determined (Table 3). In Arak, the mean temperature in January (the coldest month) is -5.7℃ (-8℃ in Hamadan as the test location) and in July (warmest month) is

35.8 ℃ (34.2 ℃ in Hamadan). The annual precipitation in Arak and Hamadan is about 307 mm and 345 mm, respectively.

Based on the Köppen climate classification, Arak and Hamadan have a continental climate. Arak is relatively cold and dry while Hamadan is cold and semi-arid. In general, apart from air pollution, weather conditions of these cities are close and thus the natural weathering is the same in both cities.

The weathering ratio (*WR*) was defined for comparing and estimating mechanical strength after the salt crystallization and natural weathering conditions. The *WR*, defined as the ratio of the average strength in natural weathering to the average strength in salt crystallization test (*SC*) in the same cycle or day (Eq. 15), was used to evaluate the extent of disintegration upon weathering (Fig. 12).

Table 3. Physico-mechanical properties of the *NCW* samples

| **G** | | | | | | **N** | | | | |
|---|---|---|---|---|---|---|---|---|---|---|
| **Day (Cycle)** | **DWL (%)** | **DVp (%)** | **σc (MPa)** | **σt (MPa)** | **Is** | **DWL (%)** | **DV (%)** | **σc (MPa)** | **σt (MPa)** | **Is** |
| 0 | 0.00 | 0.00 | 140.00 | 21.42 | 6.73 | 0.00 | 0.00 | 139.13 | 15.44 | 5.94 |
| 90 | 0.03 | 3.81 | 135.02 | 19.09 | 6.39 | 0.05 | 3.94 | 130.96 | 13.24 | 5.35 |
| 180 | 0.06 | 4.42 | 130.85 | 18.06 | 6.26 | 0.07 | 4.90 | 126.62 | 12.24 | 5.29 |
| 270 | 0.08 | 4.99 | 125.49 | 17.95 | 6.06 | 0.09 | 5.14 | 123.83 | 11.81 | 5.14 |
| 360 | 0.11 | 8.86 | 121.22 | 16.19 | 5.78 | 0.12 | 92.08 | 119.23 | 10.24 | 5.02 |
| **M** | | | | | | **Av.** | | | | |
| **Day (Cycle)** | **DWL (%)** | **DVp (%)** | **σc (MPa)** | **σt (MPa)** | **Is** | **DWL (%)** | **DV (%)** | **σc (MPa)** | **σt (MPa)** | **Is** |
| 0 | 0.00 | 0.00 | 128.97 | 12.66 | 5.91 | 0.00 | 0.00 | 136.03 | 16.51 | 6.19 |
| 90 | 0.10 | 4.03 | 125.31 | 12.44 | 5.33 | 0.06 | 3.93 | 130.43 | 14.92 | 5.69 |
| 180 | 0.17 | 5.62 | 123.70 | 12.02 | 5.16 | 0.10 | 4.98 | 127.06 | 14.11 | 5.57 |
| 270 | 0.21 | 6.68 | 119.06 | 11.66 | 5.04 | 0.13 | 5.60 | 122.79 | 13.81 | 5.41 |
| 360 | 0.12 | 8.72 | 115.80 | 11.41 | 5.00 | 0.18 | 8.84 | 117.41 | 11.41 | 5.26 |
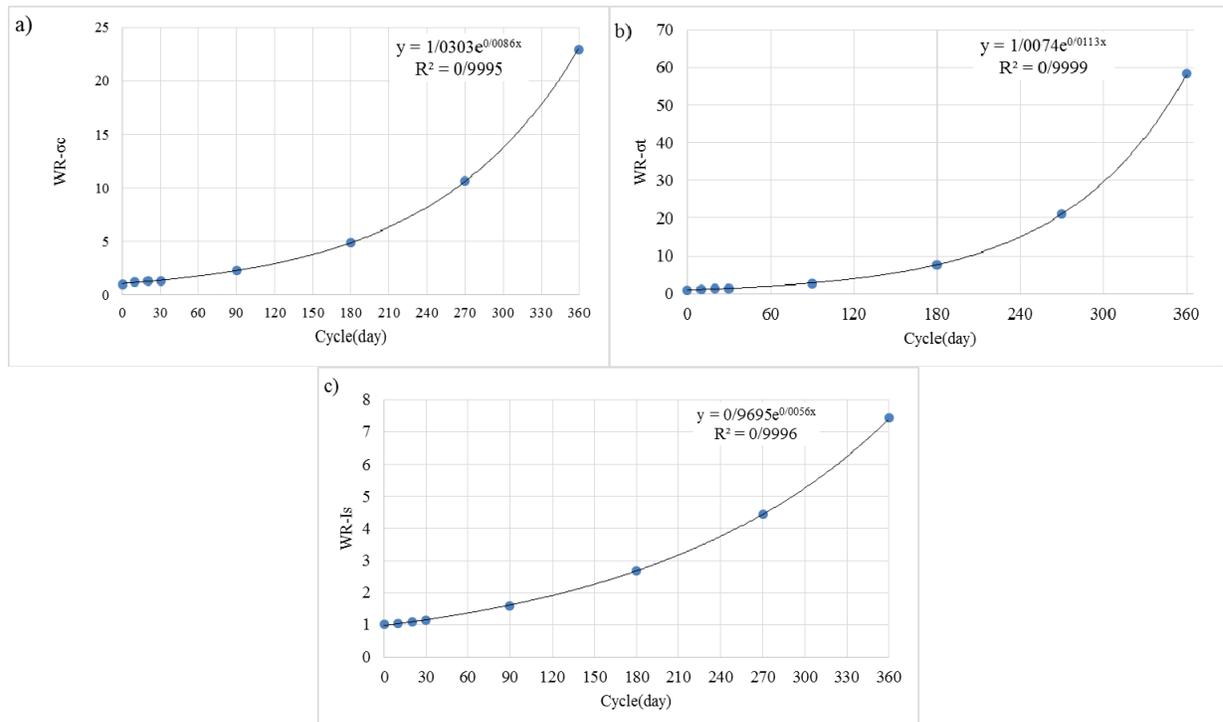


Figure 10. Relationships between *WR* and cycle (day): a) uniaxial compressive strength (*σc*), b) Brazilian test (*σt*), and c) Point load index (*Is*)

The average values were obtained using exponential Equations 6, 10, 14, 16, 17, and 18 in time intervals of 10, 20, 30, 90, 180, 270, and 360 days (cycle).

$$WR = \frac{NWC}{SC}$$       Eq. 15

$$\sigma c(Av.) = 135.89e^{-4E-04d}$$       Eq. 16

$$\sigma t(Av.) = 16.196e^{-7E-04}$$       Eq. 17

$$Is(Av.) = 6.0548e^{-4E-04d}$$       Eq. 18

Where $d$ is the day, $\sigma_c$ *(Av.)* is the average uniaxial compressive strength of the slates under natural weathering, $\sigma_t(Av.)$ is the average tensile strength of the slates under natural weathering, and *Is(Av.)* is average point load index of the slates under natural weathering. As shown in Fig. 12, after 30 cycles (day), *WR* (for *UCS*) is 1.29, suggesting that that average uniaxial compressive strength ($\sigma_c$) in natural weathering condition is 1.25 fold of average uniaxial compressive strength in salt weathering condition.

**Discussion**

Regarding the urbanization developed in Arak, use of the slates to the foundation is an inevitable issue. From a construction point of view, the slate is a rock with an unpredictable behavior that can be problematic.

In environments with high weathering potential such as urban zones (acidic and saline environment), carbonates and oxides are easily weathered such that the slate used should have at most a very small proportion of these minerals. In this regard, Arakʼs slates are considered as problematic rocks. The presence of pyrite and carbonate, beside foliation, in Arakʼs slate have urged conducting elaborate studies on weathering of these rocks. Two main causes for weathering in slate rocks are iron sulfide oxidation and gypsification, which lead to noticeable changes. These types of weathering could occur mainly in groundwater fluctuation (wetting-drying, salt crystallization, and chemical reaction), rains (chemical reaction and wetting-drying), and varying climate condition (cooling-warming, freezing-thawing, and wetting-drying). Ghadimi *et al.* (2013) demonstrated that calcareous soils and alkaline soils in Arak plain are the sources of major elements and industrial activity and traffic are the sources of heavy metals in the rainwater samples in Arak city. Because of the high groundwater level and wastewater entry, saline soils expand in the study area. Here, $Na_2SO_4$ and $NaCl$ are the main constituents of the Arakʼs brine.

Salt crystallization is the most powerful weathering agent for rocks. Rocks lose weight due to the harmful effect of salt that also causes visible surface deterioration. Many authors have described the damage caused by this salt to the volume change and hydration pressure generated when thenardite ($Na_2SO_4$) is transformed to mirabilite ($Na_2SO_4.10H_2O$). Moreover, several investigations have shown that damage due to crystallization pressure is more important than damage due to hydration pressure. Regarding saturating duration (2 h), drying duration (16 h), and drying temperature (105°C), damage from sodium sulfate due to crystallization pressure of thenardite is more possible than hydration pressure. In comparison, the pressure of mirabilite crystallization is an important parameter to decay and splitting.

Crystallization within the slates (anisotropic system) leads to the decay of their surface in the form of observable. This harmful form of crystallization (sub-florescence) is preferentially observed for sodium sulfate. Its damage caused by the internal stresses induced by the crystal pressure, combined with the growth of the crystallized zone as the stone is subjected to repeated imbibitions saturation-drying cycles, can lead to the weathering of the constitutive materials and possibly their fracture. The anisotropy elements near the external surface are the first elements to dry, resulting in a gradient of the salt thenardite, typically present in planar micropores (pores with radius < 1 mm) adjacent to fractured crystals (no mirabilite crystals were observed).

The evidence of decomposition includes peripheral edges corrosion, foliations line due to color changes (leakage of iron sulfide oxidation to foliation) or exudation, and color changes of pyrite-magnetite grain.

Laboratory testing of weathering processes is an accelerated version for the natural conditions, by which the impact of long-term weathering processes can be achieved in a very shorter span of time (White, 1976; Nara *et al.,* 2011). The samples were exposed to natural conditions, where they experienced all three climatic cycles (heating and cooling, wetting and drying, and freezing and thawing). Sun radiation, precipitation, wind blowing, and daily temperature changes lead to weathering cycles.

The calculated *WR* values reveal that salt crystallization weathering occurs more rapidly than those in natural climate condition. *WR* increases over time with an exponential trend.

The foliation has direct and indirect effects on the most physical and mechanical properties of the anisotropic rocks. Measurements show a logical relation between density (indirect relation) and porosity (direct relation) with dry weight loss and ultrasound wave velocity. The mechanical strengths also follow this trend. The average loss of physicomechanical properties of the Mesozoic's slate, in different tests and weathering conditions, show a fluctuating trend (Table 4).

Table 4 The average loss of physicomechanical properties of the Mesozoic's slate under a) salt crystallization test and b) natural weathering

a)

| Test/ Cycle | $\sigma_c$ (%) | $\sigma_t$ (%) | $I_s$ (%) | *DVp* (%) | *DWL* (%) |
|---|---|---|---|---|---|
| 10 | 16.12% | 15.14% | 7.27% | 7.86% | 0.18% |
| 20 | 19.86% | 21.28% | 11.26% | 9.63% | 0.24% |
| 30 | 23.72% | 30.93% | 15.87% | 11.52% | 0.32% |

b)

| Test/ Month | $\sigma_c$ (%) | $\sigma_t$ (%) | $I_s$ (%) | *DVp* (%) | *DWL* (%) |
|---|---|---|---|---|---|
| 3 | 4.09% | 8.95% | 8.27% | 3.93% | 0.06% |
| 6 | 6.54% | 13.82% | 10.21% | 4.98% | 0.10% |
| 9 | 9.68% | 15.87% | 12.71% | 5.60% | 0.13% |
| 12 | 12.64% | 22.23% | 15.04% | 8.84% | 0.18% |

Using calcareous slates containing pyrite-magnetite as a pavement or coverage will lead to problems in appearance (iron and magnesium oxides stains) after a while. Moreover, the bigger problem of these rocks is when they are as foundations and slopes. Water fluctuations cause salt crystallization in slates to reduce strength. As can be seen in Table 4, in a better anisotropy angle (*β*=90˚), the compressive strength was reduced about 24% (at cycle 30) whereas this amount for natural weathering condition during about 12 months is 12.64%%. This difference can be attributed to the fact that the rate of change under salt crystallization conditions is much higher than that under normal conditions. Therefore, anisotropy factor and weathering condition play key roles on negative intensity effects of weathering.

Overall, we found that slate weathering assessment still needs plenty of studies. In this connection, introducing high-performance methods to advise constructors about the material's capability uses under weathering condition is of great importance.

**Conclusions**

We showed that the rock's behaviors under weathering condition, likewise the physical and petrographic characteristics, depended on weathering situation. To assess the impacts of the process on weak and anisotropic rocks, it is necessary to have a comprehensive understanding of crystallization process. In anisotropic rocks, salt crystals become shortened depending on the degree of anisotropy, sizes of the pores, and salt composition. Sodium sulfate crystallization within the anisotropic plane (slates) leads to the adverse deterioration, which is observable. Salt crystallization is mainly seen due to fluctuations in groundwater levels. While the most important weathering parameters in atmospheric conditions (regardless of chemical reaction with air pollution) are cooling-warming, freezing-thawing, and wetting-drying. In both cases weathering processes disintegrate rocks through the existing discontinuities. In general, corrosion of edges, development of foliation's line due to color changes, color changes in pyrite-magnetite grains, appearing foliation line due to exudation and exfoliation, are apparent changes caused by weathering on the Araks' calcareous slate. As seen, slates decline occur in natural conditions, with less speed than those in laboratory weathering conditions. At the end of cycle 30 of salt crystallization, the mean weight, ultrasound wave velocity, uniaxial compressive strength ($\sigma_c$), Brazilian tensile strength ($\sigma_t$), and point load index value ($I_s$) of the samples were reduced by 0.32%, 11.52%, 23.72%, 32.15%, and 16.09%, respectively. While in natural condition, after about 12 months (360 days) these values were 0.18%, 8.84%, 12.64%, 22.23%, and 15.04%, respectively. In order to obtain more meaningful results, it is

recommended collecting in-situ rock properties under natural conditions. . In this regard, by comparing the results of laboratory weathering test with the natural weathering condition (and introduce time function), we can anticipate rock behavior under natural condition, by specific numbers of laboratory tests. Weathering ratio (*WR*) presented in this study is a parameter based on the ratio of the mechanical strength in natural weathering to the mechanical strength in salt crystallization (in the same period). This ratio is a meaningful indicator of the weathering. Based on the rock's properties and weathering condition, this ratio could be 1 to $\infty$ (Value $\infty$ is reported when the rock does not resistance to salt crystallization test).

## References

Anon, 1979. Classification of rocks and soils for engineering geological mapping. Rock and soil materials (Part 1). Bulletin International Association Engineering Geology, 19:355–371.

Cardell, C., Rivals, T., Mosquera, M.J et al., 2003. Patterns of damage in igneous and sedimentary rocks under conditions simulating sea-salt weathering. Earth Surface Processes and Landforms, 28: 1–14.

Cárdenes, V., Mateos, F., Rubio Ordoñez, A., Monterroso, C., 2012. Standard tests for the characterization of roofing slate pathologies. Materiales de Construccion, 62: 251–268.

Coussy, O., 2006. Deformation and stress from in-pore drying-induced crystallization of salt. Journal of the Mechanics and Physics of Solids, 54: 1517–1547.

Diamantis, K., Gartos, E., Migiros, G., 2014. Influence of petrographic characteristics on physic-mechanical properties of ultrabasic rocks from central Greece. Bulletin of engineering geology and the environment, 73: 1273-1292.

Fereidooni, D., Assessing the effects of mineral content and porosity on ultrasonic wave velocity, Geomechanics and Engineering. 14(4), DOI: 10.12989/gae.2018.14.4.399.

Fereidooni, D., Ghobadi, M.H., 2015. Effect of mineralogy on durability and strength of hornfelsic rocks under acidic rainfall in urban areas. Journal of Engineering Geology, 9: 2765-2788.

Fereidooni, D., Khanlari, G.H., et al., 2016. Assessment of inherent anisotropy and confining pressure influences on the mechanical behavior of anisotropic foliated rocks under triaxial compression. Rock Mechanics and Rock Engineering, 49: 2155-2163.

Gamble, J.C., 1971. Durability-Plasticity Classification of shales and other argillaceous rocks. Ph.D. Thesis, University of Illinois, Urabana, 171 pp.

Gautam, T.P., Shakoor, A., 2013. Slaking behavior of clay-bearing rocks during a one-year exposure to natural climatic conditions. Engineering Geology, 166:17–25.

Ghadimi, F., Ghomi, M., Ranjbar, M., Hajati, A., 2013. Sources of contamination in rainwater by major and heavy elements in Arak, Iran. Journal of Water Sciences Research, 5: 67-84.

Heidari, M., Torabi-Kaveh, M., Chastre, C., Ludovico-Marques, M., Mohseni, H., Akefi, H., 2017. Determination of weathering degree of the Persepolis stone under laboratory and natural conditions using fuzzy inference system. Construction and Building Materials, 145: 28–41.

Heng, S., Guo, Y., Yang, Ch., et al., 2015. Experimental and theoretical study of the anisotropic properties of shale. International Journal of Rock Mechanics & Mining Sciences, 74: 58–6.

Ikari, M.J., Niemeijer, A.R., Marone, C., 2015. Experimental investigation of an incipient shear failure in foliated rock. Journal of Structural Geology, 77: 82-91.

International Society for Rock Mechanics, 2007. In: Ulusay R, Hudson JA (eds.) Suggested Methods Prepared by the Commission on Testing Methods. Ankara, Turkey, 628 pp.

Kessler, D.W., Sligh, W.H., 1932. Physical properties and weathering characteristics of slates, Bureau of Standards Journal of Research, 9: 377-411.

Khanlari, G.R., Heidari, M., Sepahigero, A.A., Fereidooni, D., 2014. Quantification of strength anisotropy of metamorphic rocks of the Hamedan province, Iran, as determined from a cylindrical punch, point load, and Brazilian tests. Journal of Engineering Geology, 169: 80–90.

Koniorczyk, M., Gawin, D., 2012. Modeling of salt crystallization in building materials with microstructure photomechanical approach. Construction and Building Materials, 3: 6860–6873.

Lourens, A.R., PelT, L., Henk, P.H., Kopinga, K., 2005. Salt crystallization as damage mechanism in porous building materials - a nuclear magnetic resonance study. Magnetic Resonance Imaging, 23: 273–276.

Momeni, A.A., Khanlari, G.R., Heidari, M., Sepahi, A.A., Bazvand, E., 2015. New engineering geological weathering classifications for granitoid rocks. Engineering Geology, 185: 43–51.

Modestou, S., Theodoridou, M., Ioannou, I., 2015. Micro-destructive mapping of the salt crystallization front in limestone. Engineering Geology, 193: 337–347.

Nara, Y., Morimoto, K., Yoneda, T., Hiroyoshi, N., Kaneko, K., 2011. Effects of humidity and temperature on subcritical

crack growth in sandstone. International Journal of Solids and Structures, 48:1130–1140.

Rivas, T., Iglesias, J., Taboada, J., Vilán, J.A., 2011. Oxidacion de sulfurous en pizarra ornamental: tratamientos protectors con siloxanos. Materiales de Construccion, 62: 115–130.

Rodriguez-Navarro, C., Doehne, E., 1999. Salt weathering: influence of evaporation rate, supersaturation, and crystallization pattern. Earth Surface Processes and Landforms, 24:191–209.

Rodriguez-Navarro, C., Doehne, E., Sebastian, E., 2000. How does sodium sulfate crystallize? Implications for the decay and testing of building materials. Cement and Concrete Research, 30:1527–1534.

Stryszewska, T., Kanka,, S., 2017. The effects of salt crystallization in ceramic bricks in terms of line deformations. Procedia Engineering. 193: 120–127.

Walsh, J.A., 2007. The use of the scanning electron microscope in the determination of the mineral composition of Ballachulish slate. Materials Characterization, 58:1095–1103.

Ward, C., Gómez-Fernandez, F., 2003. Quantitative mineralogical analysis of Spanish roofing slates using the Relived method and X-ray powder diffraction data. European Journal Of Mineralogy, 15:1051–1062.

White, S.E., 1976. Is frost action really only hydration shattering? A review. Arctic Antarctic and Alpine Research. 8: 1–6.

Zedef, V., Doyen, K. A., Ozsen, H., Kekec, B., 2007. Effect of salt crystallization on stones of historical buildings and monuments, Konya, Central Turkey. Building and Environment journal, 42: 1453–1457.